Journal of the Korean Nuclear Society
Volume 4, Number 3, September, 1972

≪Original≫

Precipitation In Inconel 718 Alloy

Hyung Sup Choi* and Ju Choi

Korea Institute of Science and Technology, Seoul, Korea

(Received August 1, 1972)

Abstract

The precipitation sequence of Inconel 718 alloy, aged at 760°C for times up to 200 hr, has been studied by means of electron microscopy and X-ray diffraction methods. The dominant hardening phase was identified as the metastable, body-centered tetragonal Ni_3Nb phase in the morphology of platelets. The other phases identified in the aging sequence were (Nb, Ti)C and the stable acicular phase of orthorhombic Ni_3Nb.

The observations were made on the interaction of dislocations with the precipitates in the underaged condition. The shearing of the precipitates and the planar defects, *e.g.*, stacking faults on {110} planes of the intermetallic phase, were observed.

요 약

760°C에서 最高 200時間까지 時效熱處理한 Inconel 718 合金의 析出過程을 電子顯微鏡的方法과 X線廻折法으로 調査하였다.

이 合金의 主硬化相은 작은 板狀으로 된 準安定相인 體心正方系의 Ni_3Nb 相이었으며, 그밖에 判別된 析出相은 (Ni, T)C와 針狀으로 된, 安定相인 斜方系의 Ni_3Nb 相이었다.

未時效狀態에서 轉位와 析出相과의 相互作用을 觀察했으며, 그 結果 析出相의 變形과 析出相의 〔110〕面에 形成된 積層缺陷層을 觀測할 수 있었다.

1. Introduction

Inconel 718 alloy for medium temperature applications(up to 650°C) in turbine engines demonstrates high strength, good ductility and weldability. The alloy has a feature in that the strengthening of the alloy is achieved by an addition of a considerable amount of niobium, while the principal hardening elements of other nickel-base superalloys are aluminium and titanium.

On the major hardening phase in this alloy, two different phases were proposed; that is, niobium-rich face-centered cubic gamma prime precipitate and body-centered tetragonal Ni_3Nb. Eiselstein[1] identified Cu_3Au type ordered *fcc* gamma prime phase, $Ni_3(Nb, Al, Ti)$, as in most nickel-base superalloys. Recent work of Kirman and Warrington[2] has shown by analysis of electron diffraction

* Hyung Sup Choi is presently with the Ministry of Science and Technology.

patterns that the metastable strengthening phase is not *fcc* gamma prime but body-centered tetragonal structure, based on the Ni_3Nb composition. Several workers confirmed this interpretation[3,4]. On the other hand, the recent work of Barker *et al*[5] has shown by X-ray and electron microscopic examinations that the strengthening phase is *fcc* gamma prime which later transforms into metastable body-centered tetragonal Ni_xNb and finally into a stable acicular phase of orthorhombic Ni_3Nb.

In order to understand the strengthening mechanism of nickel-base superalloys, extensive work has been carried out in recent years on the deformation modes of alloys hardened with the gamma prime phase and they observed the superdislocations with particle-shearing in the underaged condition[6,7,8]. However, little information is available on the deformation of Inconel 718 alloy.

The aim of the present study was to identify the precipitated phases of Inconel 718 alloy by X-ray and electron diffraction analyses and to observe the interaction of dislocations with the precipitates.

2. Experimental Procedure

The actual weight composition of the Inconel 718 used is as follows: 0.33% C, 0.06% Mn, 0.14% Si, 19.00% Cr, 52.40% Ni, 0.21% Co, 2.94% Mo, 5.08% Nb+Ta, 0.90% Ti, 0.49% Al, 0.02% Cu and balance Fe.

The vacuum-cast alloy was homogenized for 2 hr at 1,100°C and reduced to sheets of 0.7 mm thickness by hot and cold rolling. Specimens for metallographic examination and hardness measurement were cut from the rolled sheets. All the specimens were solution treated for 4 hr at 1,130°C, followed by water quenching; helium atomsphere was provided to prevent excessive oxidation. From preliminary data, it was decided that aging at 760°C was optimum for the alloy to exhibit underaging, peak hardness and overaging states. Thus the specimens were given aging treatment for times up to 200 hr at 760°C, followed by air cooling.

For the identification of the precipitated phases by the X-ray diffraction technique, the samples were electrolytically digested using a solution of 10% phosphoric acid in water to extract finely dispersed, intragranular phases and a solution of 10% hydrochloric acid in methyl alcohol for the extraction of carbides as suggested by Kaufman and Palty[9]. The undissoved residues were separated by the centrifuge, rinsed in alcohol and then oven dried. Dried residues were examined with a Norelco X-ray diffractometer using filtered copper radiation.

For the optical metallography and the extraction replica, samples were ground through 600 grit paper and polished on a wheel with Linde B abrasive. The surfaces were then electropolished using a solution of 5% perchloric acid in acetic acid and then deeply etched anodically in an aqueous solution of 2% sulfuric acid, or alternatively, in an aqueous solution of 10% phosphoric acid. After directly depositing carbon on the etched surface, a solution of 10% hydrochloric acid in methyl alcohol was used to free the extraction replica from the surface of the specimen. For the observation of the interaction between slip lines and the precipitate, specimens were electropolished after mechanical polishing and then deformed to fracture by elongation. Carbon replicas shadowed with platinum and carbon were prepared in the same manner as described above.

Thin foils were prepared by electropolishing in a modified Bollmann apparatus using an electrolyte of chromic acid in acetic acid.

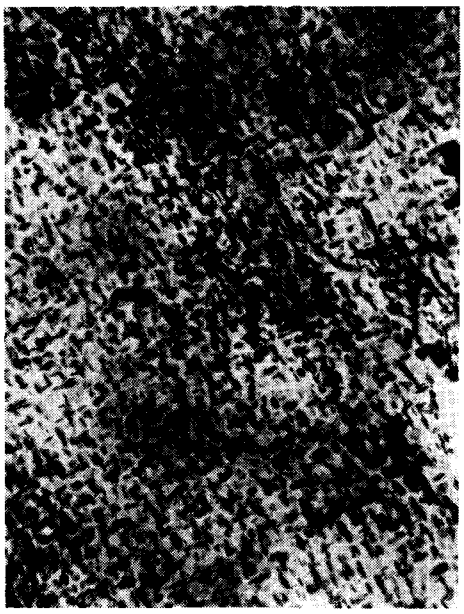

Fig. 1. Thin foil, aged for 0.5 hr at 760°C, ×32,000.

The solution was kept under 20°C during electropolishing and the current density was around 0.2 A/cm². The specimens for the electron microscopy were examined in a Hitachi HU-125C electron microscope operating at 125 kv.

3. Results

1) Phase Identification

In the specimen aged for 30 min., very finely dispersed precipitates could be detected with the electron microscope. A transmission electron micrograph Fig. 1, shows that the precipitates are substantially disc-like or platelets of around 200 Å in size. The X-ray data for residues extracted from the specimen are given in Table 1. The observed "*d*" values were in good agreement with the calculated ones based on the proposed structure of Ni_3Nb, *i.e.*, ordered, body-centered tetragonal of the Al_3Ti type, having lattice parameters $a_0=3.624$ Å, $c_0=7.406$ Å; $c/a=2.044$[2].

Fig. 2, (a) shows an electron diffraction pattern of a thin foil. It consists of weak reflections from the precipitate superimposed upon strong matrix reflections. As illustrated schematically in Fig. 2, (b), the spots could be successfully indexed as a body-centered tetragonal (114) zone according to the proposed structure. It is worthwhile to note that the allowed reflections satisfy the structure factor considerations, *i.e.*, $h+k+l=2n$ (here n denotes an integer), indicating the body-

Table 1. X-Ray data on the bct Ni_3Nb extracted from Inconel 718.

CuK$_\alpha$ Radiation

d Å	Intensities	*hkl*	$\sin^2\theta$	
			Observed	Calculated
3.2549	VVW	101	0.0561	0.0561
2.5495	M	110	0.0914	0.0905
2.0987	VS	112	0.1343	0.1338
1.8483	W	004	0.1733	0.1734
1.8072	M	200	0.1812	0.1810
1.2945	W	204	0.3554	0.3544
1.0940	VW	312	0.4965	0.4958
1.0541	VVW	224	0.5349	0.5353

* S means strong, M-medium, W-weak, V-very.

Table 2. X-Ray data on the Orthorhombic Ni_3Nb and (Nb, Ti)C.

Orthorhombic Ni_3Nb			(Nb, Ti)C		
d Å	Intensities	*hkl*	*d* Å	Intensities	*hkl*
2.637	VVW	111	2.549	VS	111
2.103	VS	020	2.212	S	200
1.989	M	021	1.566	M	220
1.965	M	211	1.336	W	311
1.528	VVW	212	1.281	W	222
1.291	M	230	1.107	VVW	400
1.271	VW	400			
1.193	VVW	023			
1.090	VVW	420			

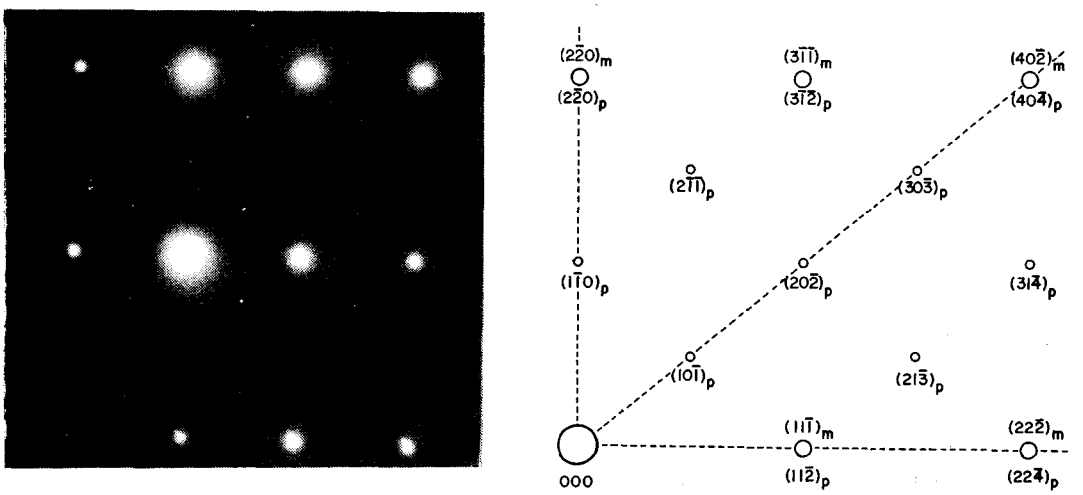

(a) (b)

Fig. 2. (a) Selected area diffraction pattern from a thin foil aged for 4 hr at 760°C: (b) Schematic reproduction of the diffraction pattern in Fig. 2, (a), zone is $(114)_p$ or $(112)_m$.

centered structure.

The coincidence of the precipitate spots with the matrix spots further indicates the fully coherent relationship between them.

The combined X-ray and electron diffaction data presented here shows the metable strengthening phase to be body-centered tetragonal in structure, isomorphous with Al_3Ti.

In the specimen aged for 96 hr, large plates forming a Widmanstätten pattern were obseved as shown in Fig. 3. Further identification of this phase was accomplished by X-ray and electron diffraction. The X-ray data for the phase are given in Table 2. It shows the acicular phase to be orthorhombic Ni_3Nb as identified by Kaufmann and Palty[9].

The electron diffraction pattern of the phase extracted from the specimen is shown in Fig. 4. It is confirmed from the pattern that the phase has an ordered, close packed, layer structure with a periodic stacking modulation of the stacking order which can be expressed as $AB'AB'\cdots\cdots$ The atomic arrangement on the close packed layer is identical with that of a one-dimensional long-peroid superlattice of $M=1$ type superstructure. The detailed interpretations of the electron diffractions obtained from the phase were given elsewhere by the authors[10].

The X-ray diffraction data given in Table 2 also shows the identification of face-centered cubic (Nb, Ti)C. This phase was found in all the specimens examined. The lattice parameter calculated from the data was 4.43 Å and it lies between the lattice parameter of 4.4702 Å for NbC[11] and that of 4.3285 Å for TiC[12], suggesting that the phase is non-stoichiometric.

2) Hardness and Microstructural Changes

Hardness The isothermal hardness curve at 760°C after solution treatment at 1,130°C for 4 hr is shown in Fig. 5. Hardness values reported here represent the average of seven or eight readings for each specimen. The maximum hardness of around DPH 270 was obtained after aging for 12 hr. The figure shows that the hardening response at this temperature is rather moderate, since the

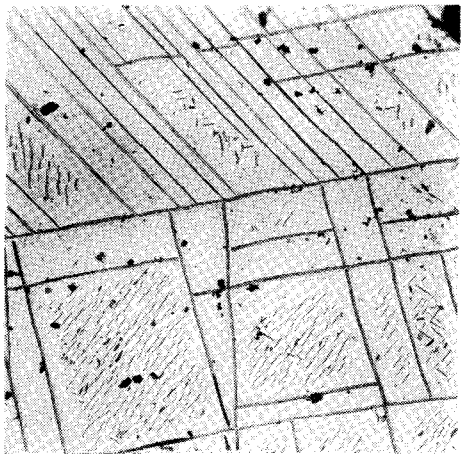

Fig. 3. Extraction replica, aged for 96 hr at 760°C, ×1,600.

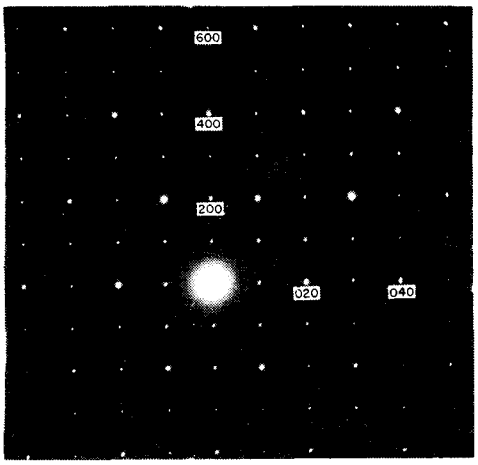

Fig. 4. Selected area diffraction pattern of the orthorhombic Ni_3Nb in the (001) orientation.

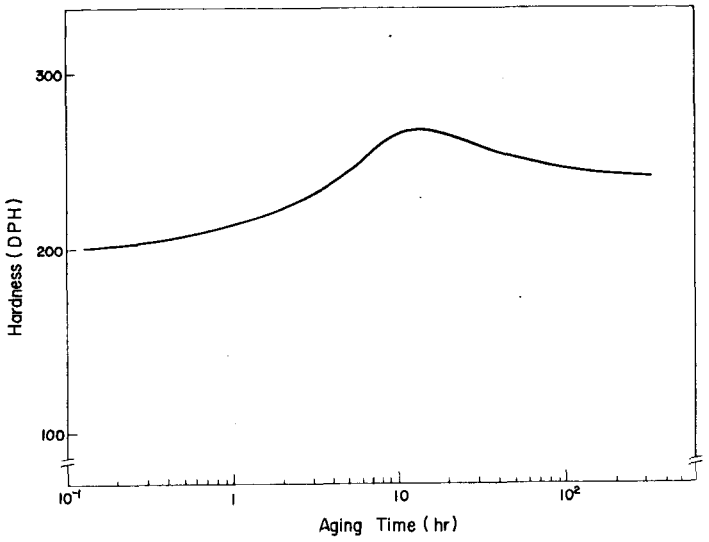

Fig. 5. The isothermal hardness curve at 760°C after solution treatment at 1,130°C for 4 hr.

peak hardness was 34% greater than the solution treatment hardness of around DPH 200.

Solution Treated Condition Specimens solution treated at 1,130°C for 4 hr were completely recrystalized with an average grain size of 0.11 mm. Many irregularly shaped particles of primary carbides were distributed in the direction of hot rolling. Occasionally, examinations of thin foils revealed a large-scale, periodic structure, termed "veining" by Sass and Cohen[13]. The direction of the veins changed abruptly on crossing grain boundaries, while no change was observed within a grain crystal, as shown in Fig. 6. It indicates that they are closely related to crystallographic directions of the grains. The contrast is obviously due to a periodic variation in the foil thickness. Sass and Cohen presumed that the structure

resulted from differential rates of dissolution of solute-rich and solute-poor regions which are spaced alternately. However, the "veining" structure is not common in the solution-treated specimens examined. Even in the same specimen, only a part of the region reveals the veining and the other part not. Therefore, it may be inferred that veining is an electropolishing artifact. Observations of similar veins were reported in a nickel-titanium alloy[13] and high-purity aluminium[14]. The veins disappeared upon aging. A thin foil electron diffraction pattern from solution treated specimens shows no superlattice reflections; it represents a pattern typical of disordered face-centered cubic solid solution.

Aged Condition In the initial stages of aging, optical examinations reveal no visible intragranular precipitates. However, electron microscopic examinations of the specimens aged for 30 min. show finely dispersed *bct* Ni_3Nb platelets within the grains. Additional aging resulted in growth of the precipitate, *e. g.*, it has grown to around 6,000 Å in size after aging for 48 hr. As aging progressed beyond 2 hr, etching attacks along slip planes were observed. An electron micrograph of Fig. 7 from the same specimen reveals that densely packed arrays of *bct* Ni_3Nb platelets are parallel to slip lines produced by the deformation of the specimens. Precipitation of the platelets along twin boundaries was also observed. Electron diffraction patterns show that the *bct* Ni_3Nb phase precipitates on {100} planes of the matrix with a growth direction of ⟨100⟩. It is interesting to note that the precipitates near grain boundaries are much smaller than those in the interior of the grains, as shown in Fig. 8.

Fig. 6. Thin foil as solution treated, vein structure, ×20,000.

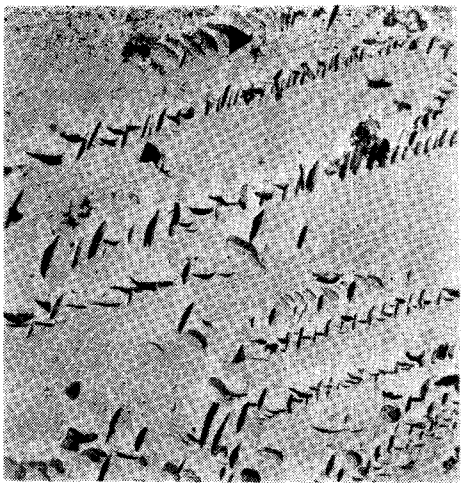

Fig. 7. Aged for 6 hr at 760°C, ×3,000.

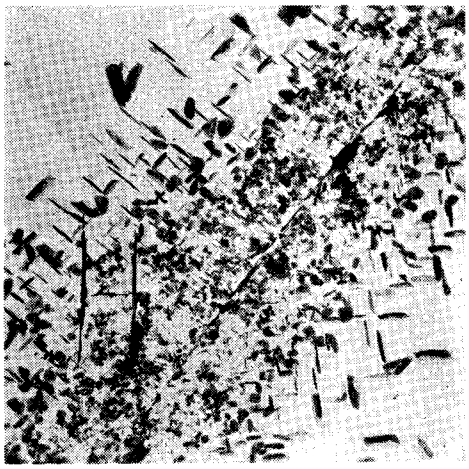

Fig. 8. Aged for 4 hr at 760°C, ×3,000.

This could have arisen from solute depletion, since it indicates that it was not able to draw excess solute from the depleted zone. Alternatively, it could be inferred that smaller platelets were precipitated later than those within the grains due to the deficiency of vacancies which would provide proper nucleation sites. However, dense precipitates near grain boundaries indicate that the latter is not probable. Further aging for 4 hr resulted in the cellular precipitation of a grain boundary phase.

In the specimen aged for 12 hr, corresponding to a peak hardness condition, the precipitates in microstructure are predominantly *bct* Ni_3Nb platelets with a few acicular phases extending from grain boundaries, as shown in Fig. 9. In the overaged condition beyond the peak hardness, *i.e.*, aged for 24 hr, a large-scale precipitation of the acicular phase was observed even with the optical microscope. Further aging caused the complete transformation to the acicular phase over the grains in a Widmanstätten pattern, with associated decrease in hardness. Observation of slip lines in Fig. 10 indicates that the plates appear to be growing on the {111} planes of the matrix and their growth direction is

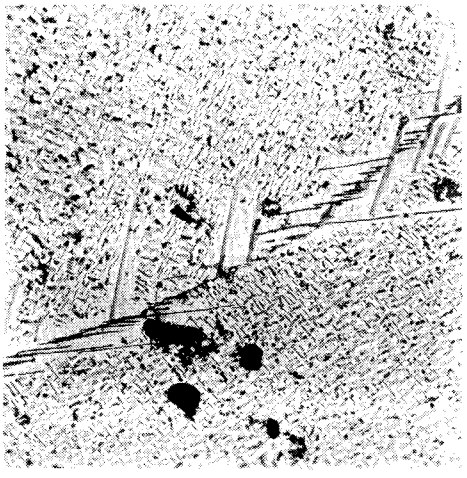

Fig. 9. Aged for 12 hr at 760°C, ×3,000.

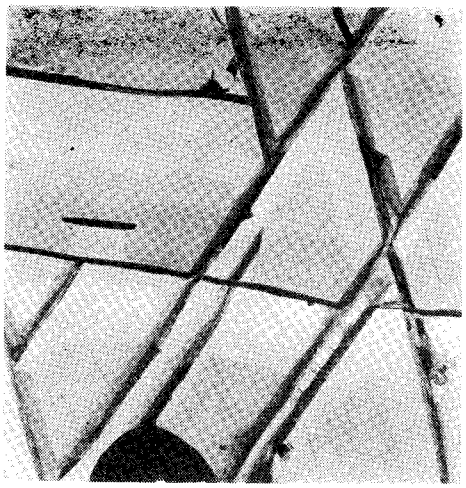

Fig. 10. Aged for 192 hr at 760°C, ×6,400.

〈110〉. After aging for 192 hr, the phase transformation of metastable *bct* Ni_3Nb to equilibrium orthorhombic Ni_3Nb was nearly completed, although there were still some coarsened metastable phases in the regions between large plates, as shown in Fig. 3.

3) Slip Structure

The slip structure of heat treated materials is similar to that observed in other nickel-base superalloys[15, 16, 17]. Fig. 11 shows a multiple slip structure of the specimen aged for 0.5 hr and deformed to fracture. Slip lines are rather inhomogeneous, containing massive displacement on widely spaced slip planes. In specimens aged for a shorter period, slip lines generally appeared to pass directly through the coherent precipitates and cause them to be deformed. Similar effects were observed in aluminium-copper alloys by Thomas and Nutting[18].

Examinations of thin foils aged for 0.5 hr revealed a coplanar array of dislocations as well as coupled pairs of dislocations, as shown in Fig. 12. It suggests that dislocations have passed directly through the precipitates. In the initial stages of aging, the coherent precipitates are so closely spaced that it requires less energy for dislocations to cut through the precipitates than to bow between them.

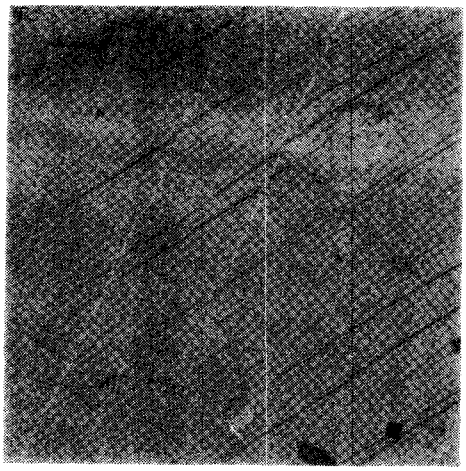

Fig. 11. Aged for 0.5 hr at 760°C, ×11,000.

Frequently, the pairs of dislocations are so widely spaced that it is difficult to judge whether dislocations are actually in pairs or not. It is supposed that loosely coupled dislocation pairs are due to short range order occurring in the matrix. The tendency of dislocations to move in pairs is gradually decreased upon aging, indicating the destruction of short range order due to the depletion of solute atoms in the matrix. Direct evidence for the deformation of the precipitates is obtained in the slightly deformed specimen aged for 2 hr, shown in Fig. 13.

From the fact that the platelets of the *bct* Ni_3Nb are in the ⟨100⟩ direction of the matrix, it is easy to see that the foil is nearly in the (001) orientation. It should be noted that two sets of planar defects with directions of ⟨110⟩ are observed in the disc-shaped precipitates lying in the (001) plane. In the deformed specimen aged for 8 hr, shown in Fig. 14, dislocations passing through the precipitates are still observed. The parallel fringes along the edges of the precipitates are displacement fringes. The dislocations piled up at the interface of the precipitates eventually cause them to be deformed, resulting in the creation of planar defects in the precipitate.

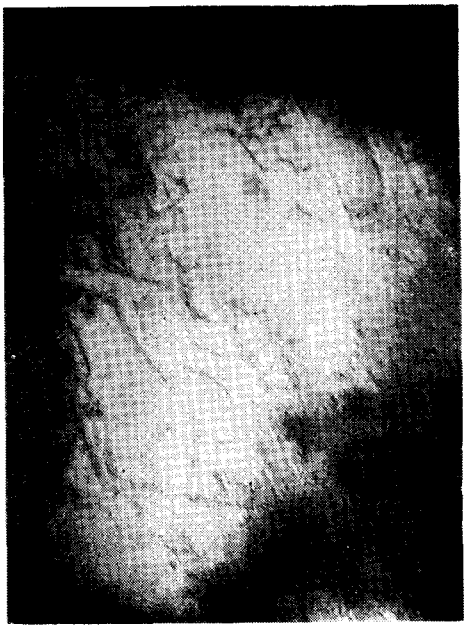

Fig. 12. Thin foil, aged for 0.5 hr at 760°C, ×26,000.

Fig. 13. Thin foil, aged for 2 hr at 760°C, ×11,000.

In the initial precipitation stages of the acicular, orthorhombic Ni_3Nb phase, slip lines appeared to pass through the phase, indicating that the acicular phase remains coherent or at

Fig. 14. Thin foil, aged for 8 hr at 760°C, ×27,000.

least partially coherent with the matrix. When the plate has grown in the overaged condition, slip lines are frequently stopped at the interface even at large strains, suggesting the loss of the coherency state of the precipitate with the matrix. From the above observations, it may be concluded that the initial hardening response can be understood as the process of cutting the coherent precipitates by dislocations.

4. Discussion

The results of the investigation presented here show the major hardening phase of Inconel 718 alloy to be *bct* Ni_3Nb which is coherent with the matrix. This metastable phase transforms to orthorhombic Ni_3Nb upon overaging.

In the recent work of Barker *et al.*,[5] the *fcc* gamma prime phase was identified as the strengthening phase which later transformed to *bct* Ni_xNb and then to orthorhombic Ni_3Nb. Further, they report that the morphology of individual phases are definitely distinguished, *i.e.*, *fcc* gamma prime, *bct* Ni_xNb, and orthorhombic Ni_3Nb were in the shapes of spheroidal or disc-like platelets, small plates, and large plates. respectively.

In order to confirm the gamma prime phase, electron microscopic observations were made on the residues extracted from short-time aged specimens. Residues were dispersed on the grid coated with carbon film. Large clusters were removed by tapping or shaking. The morphology of the extracted phases in a solution of 2% sulfuric acid in water consisted of needles and disc-like particles and no spheroidal particles were observed. Frequently, it was quite possible to obtain a selected area diffraction pattern from a disc-like particle which was fully separated from the small clusters of needles and disc-like particles. An extensive comparision was made on "*d*" spacings calculated from electron diffraction patterns obtained both from a disc-like platelet and a small cluster of disc-like and needles. The result showed no difference between them and it was also in good agreement with that of X-ray diffraction.

In view of the above results, it may be concluded that needles and disc-like particles are all *bct* in structure and the needles are actually "edgeon" views of the disc-shaped precipitates. Since there are no unique superlattice reflections for the *fcc* gamma prime phase when *bct* Ni_3Nb is present, the techniques described by Paulonis *et al*[19] should be employed to identify the *fcc* phase. With this technique, no gamma prime precipitate was found. However, the results obtained here do not excluded the possibility of the presence of the gamma prime phase. As suggested by Quist *et al*,[20] the absence of the *fcc* phase is probably due to the relatively higher temperature of aging employed in this investigation.

The transformation mechanism of *bct* Ni_3Nb to orthorhombic Ni_3Nb is not definitely

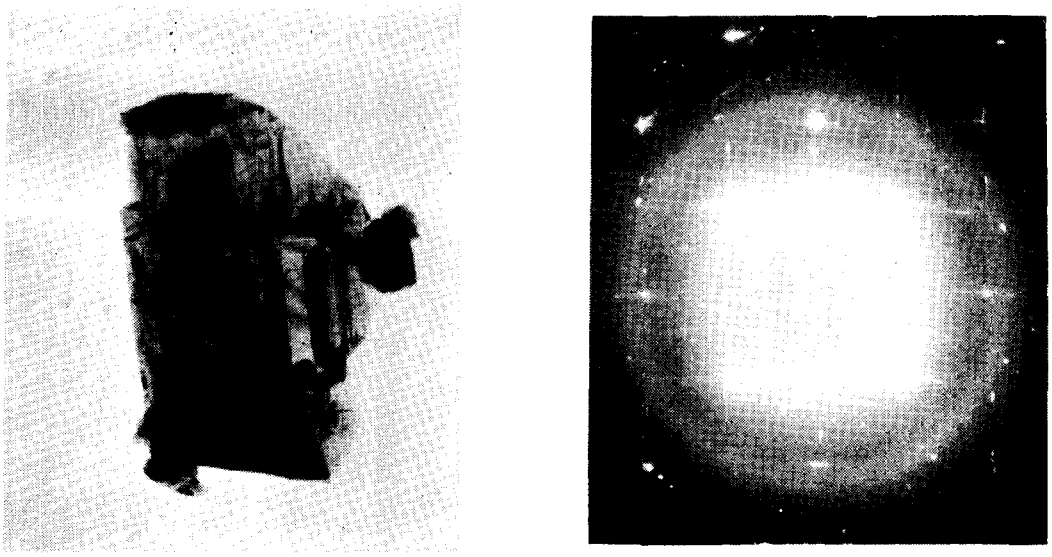

(a) (b)

Fig. 15. (a) Electron micrograph of a platelet extracted from a specimen aged for 4 hr at 76°C, ×18,000. (b) Selected area diffraction pattern of a platelet in Fig. 15, (a).

Fig. 16. Deformed platelet aged for 12 hr at 760°C.

known. However, the most likely mode seems to be that orthorhombic Ni_3Nb plates are reprecipitated after dissolution of *bct* Ni_3Nb platelets, since the areas adjacent to the large plates of orthorhombic Ni_3Nb were usually devoid of *bct* Ni_3Nb platelets, as can be seen in Fig. 9

Planar defects in the disc-shaped precipitates were frequently observed in the deformed specimens as mentioned previously. A limited electron diffraction work was performed in order to clarify the nature of defects Fig. 15, (a) shows the two sets of planar defects in the extracted precipitate and Fig. 15, (b) shows a selected area electron diffraction pattern from the same precipitate. The reflections are streaked in direction normal to the striations. The streaks indicate the formation of planar faults on [110] planes of the intermetallic phase. Extra spots due to double diffraction were frequently observed but no twin reflections were observed.

Koda *et al*[21, 22], observed similar striations in θ' precipitates of Al-Cu alloy and they concluded that striations are dislocations lying on the interface of precipitates or moire fringes resulting from these dislocations. However, Kajiwara[23] concluded that striations are due to stacking faults. In the case of this investigation, no moire fringes were observed. Thus the striations appear to arise from stacking faults, as shown

in Fig. 16, which exhibits the fringe typical of a stacking fault.

The occurence of stacking faults may be caused by the motion of partial dislocations in the precipitate, since the precipitate has a lower stacking fault energy than the matrix, which promotes deformation by this mode. Work is now in progress to define the true structure of planar defects and the results will be given elsewhere.

5. Conclusions

The experimental results led to the following conclusions:

1) The identification of the phases of Inconel 718 alloy, aged isothermally at 760°C was accomplished by electron and X-ray diffraction methods. The phases identified were (Nb, Ti)C, body-centered tetragonal Ni_3Nb and orthorhombic Ni_3Nb.

2) The dominant strengthening phase was the body-centered tetragonal Ni_3Nb in the form of platelets, which transformed into plates of orthorhombic Ni_3Nb in the overaged condition.

3) In view of the observations made on the interaction of dislocations as well as slip lines with the precipitates, the initial hardening response in the underaged condition can be understood as the process of cutting the coherent precipitate by dislocations.

Acknowledgement

The work was sponsored by the Ministry of Science and Technology, Korea. To the Ministry grateful acknowledgement is made for the financial support which has given the opportunity to perform this investigation. The authors also wish to express their gratitude to the late K. S. Shim and Soo Chul Kim who assisted us in performing the work.

References

1) Eiselstein, H. L., ASTM. Spec. Tech. Pub., **369**, 62 (1965)
2) Kirman, I., and D. H. Warrington, J. Iron Steel Inst., **205**, 1264 (1967)
3) Raymond, E. L., Trans. AIME., **239**, 1415(1967)
4) Kotval, P. S., Trans. AIME., **242**, 1764 (1968)
5) Barker, J. F., E. W. Ross, and J. F. Radavich, J. Metals, **22**, 31 (1970)
6) Hornbogen, E., and M. Mukherjee, Z. Metallk., **55**, 293 (1964)
7) Gleiter, H., and E. Hornbogen, Phys. Status Solidi, **12**, 251 (1965)
8) Kear, B. H., G. R. Leverant and J. M. Oblak, Trans. ASM., **62**, 639 (1969)
9) Kaufman, M., and A. E. Palty, Trans. AIME., **221**, 1253 (1961)
10) Choi, H. S., and J. Choi, J. Kor. Inst. Metals, **10**, 8 (1972)
11) Amendola, A., See ASTM Card File, No. 10-181, (1958)
12) See ASTM Card File, No. 6-0614.
13) Sass, S. L., and J. B. Cohen, Trans. AIME., **245**, 153 (1969)
14) Froment, M., J. Microscop., **4**, 285 (1965)
15) Copley, S. M., and B. H. Kear, Trans. AIME., **239**, 984 (1967)
16) Piearcey, B. J., B. H. Kear, and R. W. Smashey, Trans. ASM., **60**, 634 (1967)
17) Choi, H. S., and J. Choi, J. Kor. Nucl. Soc., **2**, 163 (1970)
18) Thomas, G., and J. Nutting, J. Inst. Metals, **86**, 7 (1957-1958)
19) Paulonis, D. F., J. M. Oblak, and D. S. Duvall, Trans. ASM., **62**, 611 (1969)
20) Quist, W. E., R. Taggart, and D. H. Polonis, Met. Trans., **2**, 825 (1971)
21) Koda, S., K. Matsuura, and S. Takahashi, J. Inst. Metals, **91**, 229 (1962-63)
22) Koda, S., K. Matsuura, and N. Nemoto, J. Australian Inst. Metals, **8**, 197 (1963)
23) Kajiwara, S., J. Phys. Soc. Japan, **26**, 339 (1963)